Supplementary Materials

Rational Electrolyte Formulation for Sodium Metal Batteries Operating in Extremely Cold Environments

Chuanlong Wang, Peiyu Wang, and Weiyang Li *

Thayer School of Engineering, Dartmouth College, Hanover, NH 03755, USA; weiyang.li@dartmouth.edu
Received: 3 March 2026; Revised: 27 March 2026; Accepted: 30 March 2026; Published: 31 March 2026

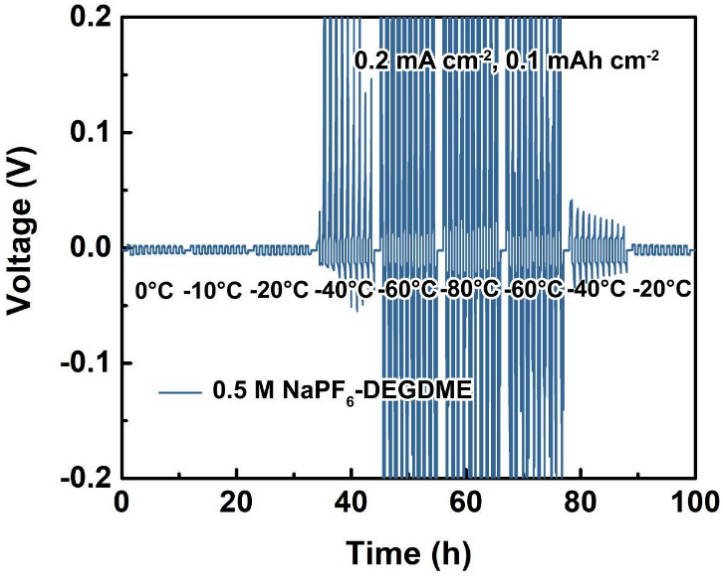

Figure S1. Galvanostatic cycling of Na || Na symmetric cells at 0.2 mA cm^{-2} and 0.1 mAh cm^{-2} in an electrolyte composed of 0.5 M $NaPF_6$-DEGDME.

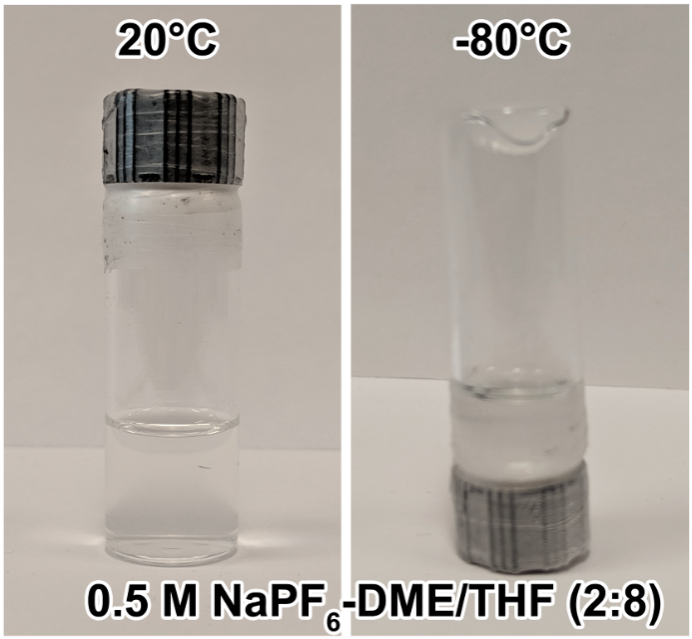

Figure S2. Photos of 0.5 M NaPF6-DME/THF (2:8) after storing at 20 °C and −80 °C for 24 h (Salt precipitation was observed at the bottom of the vial at −80 °C).

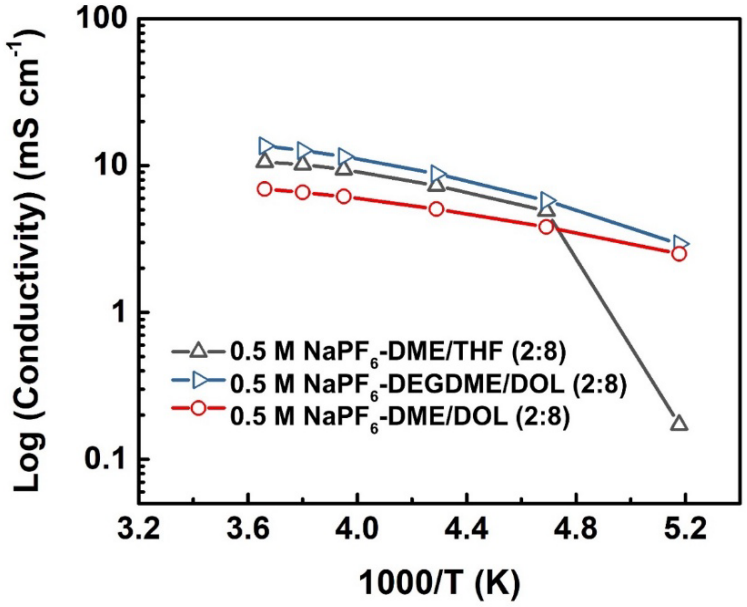

Figure S3. Temperature dependent ionic conductivity of 0.5 M $NaPF_6$-DME/THF (2:8), 0.5 M $NaPF_6$-DEGDME/DOL (2:8) and 0.5 M $NaPF_6$-DME/DOL (2:8).

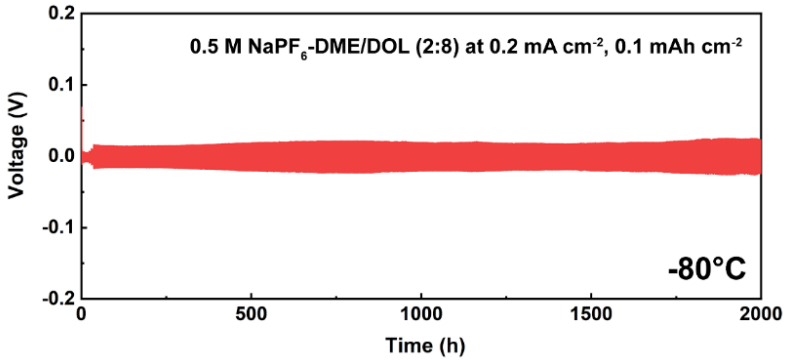

Figure S4. Galvanostatic cycling of Na || Na symmetric cells at 0.2 mA cm^{-2} and 0.1 mAh cm^{-2} at −80 °C. Note that initial stepwise temperature drop was carried out to stabilize the cells.

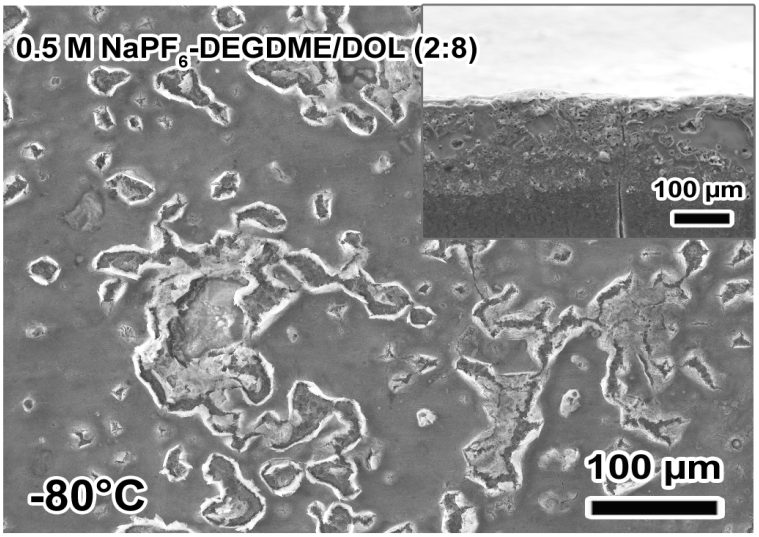

Figure S5. SEM image of Na metal surface after 50 cycles in 0.5 M $NaPF_6$-DEGDME/DOL (2:8) at −80 °C (Inset: corresponding cross-sectional SEM image).

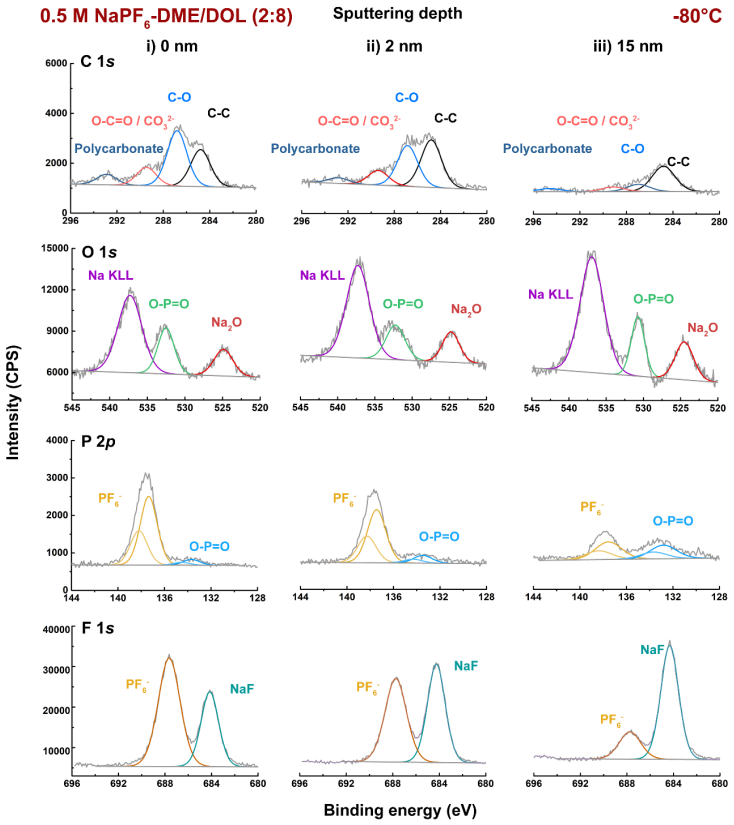

Figure S6. XPS depth profile analysis on the Na metal electrode after 50 cycles (symmetric Na || Na cells) at a current density of 0.5 mA cm^{-2} with a capacity of 0.5 mAh cm^{-2} in 0.5 M $NaPF_6$-DME/DOL (2:8) electrolyte at −80 °C.

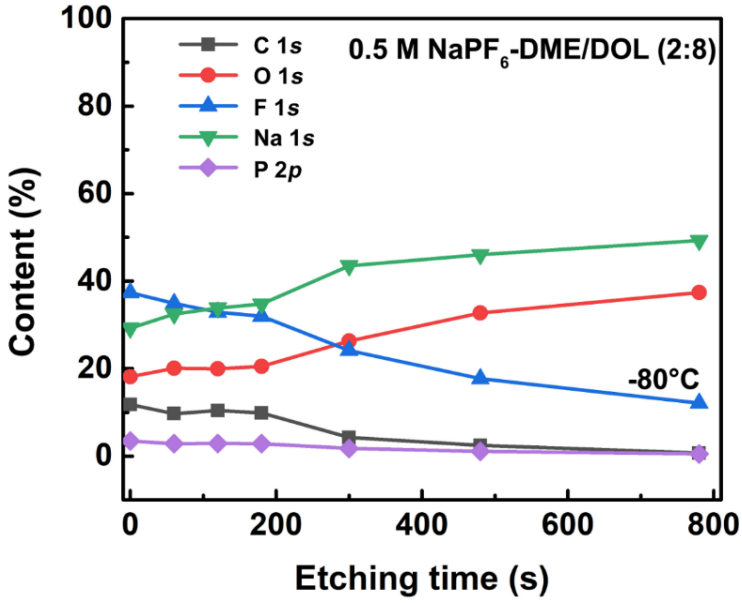

Figure S7. Contents of elements determined by ex-situ postmortem XPS depth profiling of the Na metal electrode (symmetric Na || Na cells) in 0.5 M $NaPF_6$-DME/DOL (2:8) after cycling at −80 °C.

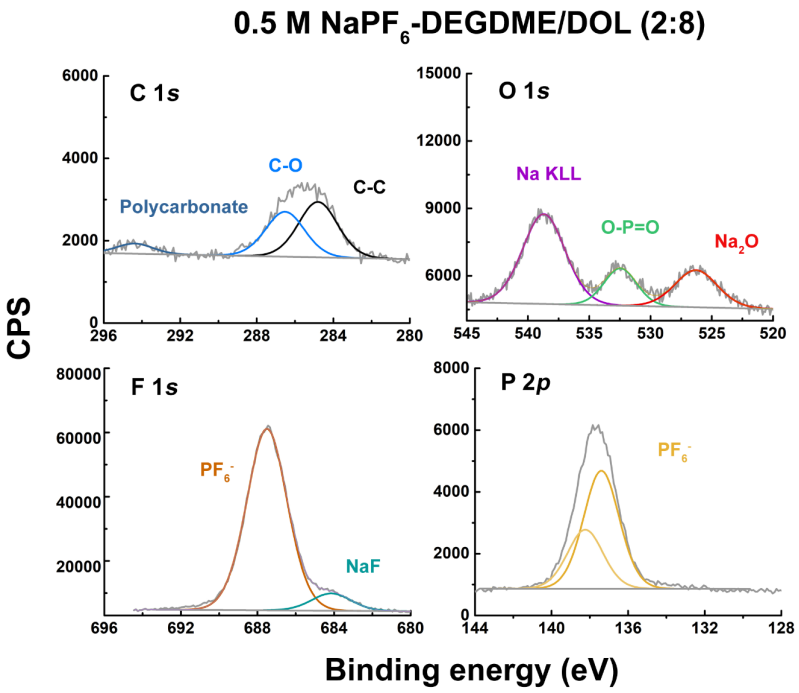

Figure S8. XPS profiles of C 1*s*, O 1*s*, F 1*s* and P 2*p* of the Na metal surface after 50 cycles (symmetric Na || Na cells) in 0.5 M $NaPF_6$-DEGDME/DOL (2:8) at 0.5 mA cm^{-2} and 0.5 mAh cm^{-2} at −80 °C.

Table S1. Summary comparing performance of Na metal anodes (symmetric cells of Na/Na) cycling at current density ≥0.5 mA cm^{-2} and at low temperatures (≤40 °C).

System	Temperature (°C)	Current (mA cm^{-2})	Capacity (mAh cm^{-2})	Overpotential (mV)	Cycle number	Ref.
Na/Na	−80	0.5	0.25	54	>1460	This work
Na/Na	−40	1.0	1.0	16	>375	This work
Na/Na	−40	1.0	3.0	16	10	This work
Na/Na	−40	3.0	1.0	82	10	This work
Na/Na	−40	1.0	1.0	~110	>165	[1]
Na/Na	−80	0.5	0.25	~150	>715	[1]
Na/Na	−60	0.5	0.25	~200	10	[2]
Na/Na	−40	0.5	1.0	~40	5	[3]
Na/Na	−40	0.5	1	~50	10	[4]
Na/Na	−60	0.5	0.5	~130	5	[5]

Table S2. Melting point, dielectric constant, and dynamic viscosity of DEGDME, DME, DOL and THF [1–3,6].

Solvent	Melting Point (°C)	Dielectric Constant (ε) at 25 °C	Dynamic Viscosity (η) (mPa·S) at −35 °C
DEGDME	−64	7.30	2.34
DME	−58	7.20	1.89
DOL	−95	7.00	1.82
THF	−108.4	7.58	0.49

Table S3. Summary of $NaPF_6$ salt dissolution in binary solvents at 0.5 M concentrations at −35 °C ("Yes" indicates fully dissolved; "No" indicates not fully dissolved; "Partially" indicates slight solid precipitation as the electrolyte approached its saturation point; "*" indicates the six electrolytes systems that were selected for the further electrochemical evaluation).

Electrolyte Composition	Solubility
***0.5 M $NaPF_6$-DME:DOL (8:2)**	**Yes**
***0.5 M $NaPF_6$-DME:DOL (5:5)**	**Yes**
***0.5 M $NaPF_6$-DME:DOL (2:8)**	**Yes**
0.5 M $NaPF_6$-DME:THF (8:2)	No
0.5 M $NaPF_6$-DME:THF (5:5)	No

Table S3. *Cont*.

Electrolyte Composition	Solubility
***0.5 M $NaPF_6$-DME:THF (2:8)**	**Yes**
0.5 M $NaPF_6$-DEGDME:DOL (8:2)	Yes
0.5 M $NaPF_6$-DEGDME:DOL (5:5)	Yes
***0.5 M $NaPF_6$-DEGDME:DOL (2:8)**	**Yes**
0.5 M $NaPF_6$-DEGDME:THF (8:2)	No
0.5 M $NaPF_6$-DEGDME:THF (5:5)	Partially
***0.5 M $NaPF_6$-DEGDME:THF (2:8)**	**Yes**

Table S4. Summary of identified XPS peaks [7–11].

C_{1s} (eV)	O_{1s} (eV)	F_{1s} (eV)	P_{2p} (eV)
Polycarbonate (293) O-C=O/CO_3^{2-} (289.5) C-O (286.8) C-C (284.8)	Na KLL (537) O-P=O (532.5) Na_2O (526)	PF_6^- (687.6) Na-F (684.2)	PF_6^- (137.4) O-P=O (133.7)

NOTE: XPS positions in P_{2p} spectra are based on $2p_{3/2}$. For XPS peak-fitting of P_{2p}, $2p_{3/2}$ to $2p_{1/2}$ area ratio is fixed at 2:1 according to the ratio of degeneracy, where 0.84 eV is employed as the doublet separation of $2p_{3/2}$ and $2p_{1/2}$.

References

1. Wang, C.; Thenuwara, A.C.; Luo, J.; Shetty, P.; McDowell, M.; Zhu, H.; Posada-Pérez, S.; Xiong, H.; Hautier, G.; Li, W. Extending the low-temperature operation of sodium metal batteries combining linear and cyclic ether-based electrolyte solutions. *Nat Commun.* **2022**, *13*, 4934.
2. Thenuwara, A.C.; Shetty, P.; Kondekar, N.; Wang, C.; Li, W.; McDowell, M. Enabling highly reversible sodium metal cycling across a wide temperature range with dual-salt electrolytes. *J. Mater. Chem. A* **2021**, *9*, 10992–11000.
3. Hu, X.; Matios, E.; Zhang, Y.; Wang, C.; Luo, J.; Li, W. Deeply cycled sodium metal anodes at low temperature and in lean electrolyte conditions. *Angew. Chem. Int. Ed.* **2021**, *60*, 5978–5983.
4. Ge, B.; Deng, J.; Wang, Z.; Liang, Q.; Hu, L.; Ren, X.; Li, R.; Lin, Y.; Li, Y.; Wang, Q. et al. Aggregate-Dominated Dilute Electrolytes with Low-Temperature-Resistant Ion-Conducting Channels for Highly Reversible Na Plating/Stripping. *Adv. Mater.* **2024**, *36*, 2408161.
5. Zhou, J.; Wang, Y.; Wang, J.; Liu, Y.; Li, Y.; Chen, L.; Ding, D.; Dong, S.; Zhu, Q.; Tang, M. et al. Low-temperature and high-rate sodium metal batteries enabled by electrolyte chemistry. *Energy Storage Mater.* **2022**, *50*, 47–54.
6. Aminabhavi, T.; Gopalakrishna, B. Density, viscosity, refractive index, and speed of sound in aqueous mixtures of N,N-dimethylformamide, dimethyl sulfoxide, N,N-dimethylacetamide, acetonitrile, ethylene glycol, diethylene glycol, 1,4-dioxane, tetrahydrofuran, 2-methoxyethanol, and 2-ethoxyethanol at 298.15 K. *J. Chem. Eng. Data* **1995**, *40*, 856–861.
7. Moulder, J.F. *Handbook of X-ray Photoelectron Spectroscopy: A Reference Book of Standard Spectra for Identification and Interpretation of XPS Data*; Physical Electronics Division, Perkin-Elmer Corporation Press: Eden Prairie, MI, USA, 1992.
8. Seh, Z.; Sun, J.; Sun, Y.; Cui, Y. A highly reversible room-temperature sodium metal anode. *ACS Cent. Sci.* **2015**, *1*, 449–455.
9. Fiedler, C.; Luerssen, B.; Rohnke, M.; Sann, J.; Janek, J. XPS and SIMS analysis of solid electrolyte interphases on lithium formed by ether-based electrolytes. *J. Electrochem. Soc.* **2017**, *164*, A3742–A3749.
10. Lutz, L.; Corte, D.; Tang, M.; Salager, E.; Deschamps, M.; Grimaud, A.; Johnson, L.; Bruce, P.; Tarascon, J. Role of electrolyte anions in the Na–O_2 battery: Implications for NaO_2 solvation and the stability of the sodium solid electrolyte interphase in glyme ethers. *Chem. Mater*. **2017**, *29*, 6066–6075.
11. Wang, H.; Wang, C.; Matios, E.; Li, W. Facile stabilization of the sodium metal anode with additives: Unexpected key role of sodium polysulfide and adverse effect of sodium nitrate. *Angew. Chem. Int. Ed.* **2018**, *57*, 7734–7737.